JOURNAL OF VIROLOGY, May 1997, p. 3397–3406 Vol. 71, No. 5
0022-538X/97/$04.00+0

Mutations in the Kissing-Loop Hairpin of Human Immunodeficiency Virus Type 1 Reduce Viral Infectivity as well as Genomic RNA Packaging and Dimerization

MICHAEL LAUGHREA,[1,2]* LOUIS JETTÉ,[1] JOHNSON MAK,[1,2] LAWRENCE KLEIMAN,[1,2] CHEN LIANG,[1,2] AND MARK A. WAINBERG[1,2,3]

McGill AIDS Centre, Lady Davis Institute for Medical Research, Sir Mortimer B. Davis-Jewish General Hospital,[1] and Departments of Medicine[2] and Immunology and Microbiology,[3] McGill University, Montreal, Quebec, Canada

Received 21 October 1996/Accepted 30 January 1997

A stem-loop termed the kissing-loop hairpin is one of the most highly conserved structures within the leader of human immunodeficiency virus type 1 (HIV-1) and chimpanzee immunodeficiency virus genomic RNA. Because it plays a key role in the in vitro dimerization of short HIV-1 RNA transcripts (M. Laughrea and L. Jetté, Biochemistry 35:1589–1598, 1996, and references therein; M. Laughrea and L. Jetté, Biochemistry 35:9366–9374, 1996, and references therein) and because dimeric RNAs may be preferably encapsidated into the HIV-1 virus, alterations of the kissing-loop hairpin might affect the in vivo dimerization and encapsidation processes. Accordingly, substitution and deletion mutations were introduced into the kissing-loop hairpin of an infectious HIV-1 molecular clone in order to produce viruses by transfection methods. The infectivity of the resulting viruses was decreased by at least 99%, the amount of genomic RNA packaged per virus was decreased by 50 to 75%, and the proportion of dimeric genomic RNA was reduced from >80 to 40 to 50%, but the dissociation temperature of the genomic RNA was unchanged. There is evidence suggesting that the deletion mutations moderately inhibited CAp24 production but had no significant effect on RNA splicing. These results are consistent with the kissing-loop model of HIV-1 RNA dimerization. In fact, because intracellular viral RNAs are probably more concentrated in transfected cells than in cells infected by one virus and because the dimerization and encapsidation processes are concentration dependent, it is likely that much larger dimerization and encapsidation defects would have been manifested within cells infected by no more than one virus.

The primer binding site and the *gag* gene of human immunodeficiency virus type 1 (HIV-1) genomic RNA are separated by 136 nucleotides extending from U200 to G335 in HIV-1_{Lai}. This 3′ half of the leader is called the L sequence (14). It has the potential to fold into three hairpins, the kissing-loop domain (KLD), the 5′ splice junction hairpin (SD), and hairpin 3 (Fig. 1). The KLD, located in the middle of the L sequence, encompasses a stem-loop, named the kissing-loop hairpin (nucleotides [nt] 248 to 270 [Fig. 1]), seated on top of a short but completely conserved stem-bulge (Fig. 1). In all HIV-1 and chimpanzee immunodeficiency viruses (SIV_{cpz}) for which published L sequences are available, the kissing-loop hairpin is characterized by a 7-bp stem (stem C) and an 8- to 9-nt loop (loop C) containing the autocomplementary sequence GCGC GC262 or GUGCAC262 (Fig. 1 and 2). Within the HIV-1/SIV_{cpz} lineage, the KLD seems to be the most conserved region of the L sequence (Table 1). It is better conserved, for example, than the region centered on hairpin 3 which has been implicated, together with other regions (7, 9, 31, 47, 59, 70), in genomic RNA packaging (1, 11, 30, 44, 49). As the most highly conserved sequence located halfway between the primer binding site and the AUG336 initiation codon of the *gag* gene and only 30 nt upstream of the 5′ splice junction, the KLD may play an important role in HIV-1 replication.

The kissing-loop hairpin deserves in vivo scrutiny for four additional reasons. (i) Both mutating loop C (Fig. 1) to a nonautocomplementary sequence (13, 67) and deleting the 5′ (38) or 3′ strand (39) of stem C (Fig. 1) have been shown to annihilate the dimerization potential of HIV-1 RNA transcripts coding for the first 500 to 1,000 nt of HIV-1 genomic RNA. These findings, together with the fact that all retroviral genomes are formed of two identical RNAs noncovalently linked near their 5′ ends (3, 4, 37, 54), strongly suggest that the role of the kissing-loop hairpin in the in vivo genomic RNA dimerization process should be investigated. (ii) The kissing-loop hairpin overlaps with a region (the 241-to-253 sequence) whose replacement by a 13-base linker appeared to reduce genomic RNA encapsidation by 78 to 85% (Fig. 1) (33). (iii) Since 1994, at least 14 important papers documenting a crucial role for kissing-loop hairpins in the in vitro dimerization of relatively short RNA transcripts from HIV-1 (13, 38–40, 51–53, 57, 58, 66, 67), Moloney murine leukemia virus (22, 23), and avian sarcoma-leukosis virus (19) have been published. (iv) It has been hypothesized that genomic RNA dimerization is a prerequisite for packaging (20).

The purpose of this study was to investigate whether mutations of the kissing-loop hairpin, introduced into an infectious HIV-1 molecular clone, affect the genomic RNA dimerization and packaging of HIV-1 viruses produced from transfected cells. The results suggest that mutations of the kissing-loop hairpin, though they reduce viral infectivity by at least 99%, have moderate (but real) effects on genomic RNA dimerization and packaging, as well as CAp24 production, but little effect on RNA splicing. It is argued that the effect of the mutations on dimerization and packaging in the cytoplasm of a cell infected at the lowest possible multiplicity of infection should be greater than that in transfected cells.

* Corresponding author. Mailing address: Lady Davis Institute for Medical Research, 3755 Cote Ste. Catherine Rd., Montreal, Quebec H3T 1E2, Canada. Phone: (514) 340-8260. Fax: (514) 340-7502.

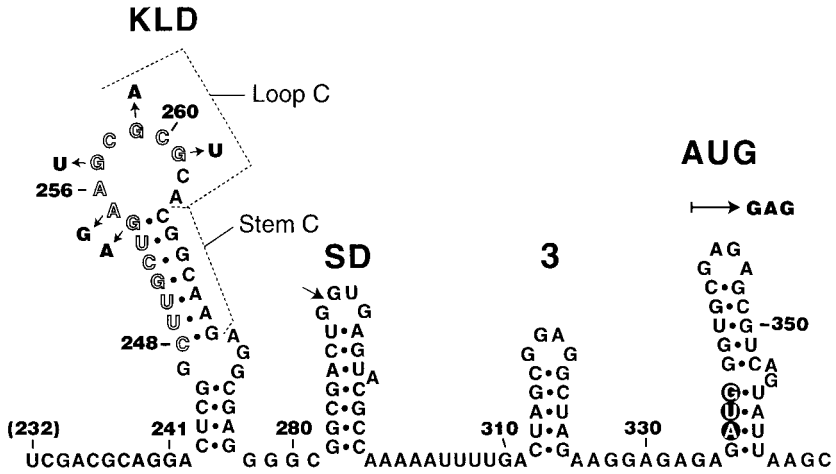

FIG. 1. Secondary RNA structure model for the HIV-1_{Lai} L sequence. The cleavage site within the 5′ major splice donor is marked by an arrow within the SD hairpin. The AUG initiation codon of the *gag* gene is circled and somewhat arbitrarily presented as hydrogen bonded for compactness. This model is based on published structure probing and/or phylogenetic data (2, 5, 12, 29, 31, 38, 63). The data of each group either directly support or are consistent with this model. The point mutations introduced into the ACS$^-$ mutant are indicated by arrows within the KLD, the nucleotides deleted in the Δ248-261 mutant are shown as open letters, and the first and last nucleotides of the Δ241-256 mutant are numerically pointed out.

MATERIALS AND METHODS

Buffers. Buffer TNE consisted of 20 mM Tris (pH 7.5), 100 mM NaCl, and 1 mM EDTA. Buffer L (38, 48) consisted of 50 mM sodium cacodylate (pH 7.5), 40 mM KCl, and 0.1 mM $MgCl_2$. Buffer H (38, 48) consisted of 50 mM sodium cacodylate (pH 7.5), 300 mM KCl, and 5 mM $MgCl_2$. Buffer TBE_2 (61) consisted of 89 mM Tris, 89 mM borate, and 2 mM EDTA. Buffer TBM (38, 42) was the same as buffer TBE_2 with EDTA replaced by 1 mM $MgCl_2$.

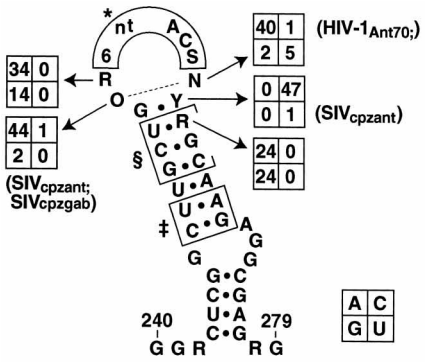

FIG. 2. Secondary structure model of the KLDs of 48 viruses from the HIV-1/SIV_{cpz} lineage for which published sequences of the region of interest are available (10, 21, 55, 64, 69). When the primary structure is not completely conserved, the number of times a given nucleotide is found at a given position is displayed in an adjacent box divided into quadrants, one for each nucleotide. When a nucleotide choice occurs in only one viral sequence, the name of the sequence is indicated next to the relevant box. Because a majority of published L sequences come from non-replication-competent strains and because sequencing mistakes are always possible (43), we judged that blind acceptance of every nucleotide assessment would be a mistake. Forty-eight sequences, including sequences from HIV-1 subtypes A, B, C, D, E, F, G, O, and U as well as the sequences of all replication-competent HIV-1 strains, were accepted. Two sequences were somewhat arbitrarily excluded. HIV-1_{oyi} was excluded on the basis of its avirulence and its 6-bp stem C (32). The CxC mismatch in the middle of stem C of HIV-$1_{3202a21}$ was dismissed either as a sequencing mistake or as related to the non-syncytium-inducing character of the clone in question. (HIV-$1_{3202a12}$, a syncytium-inducing clone isolated from the same patient, has a regular stem C [26].) Finally, a mistake in the database sequence of the KLD of HIV-1_{Hxb2} has previously been corrected (39). *, 6-nt-long autocomplementary sequence (27GCGCGC for 21GUGCAC); §, in this 3-bp box, U-R, C-G, and G-C replaced by C-G, G-C, and A-U, respectively, in HIV-1_{Ant70}; ‡, this 2-bp box underwent a transition in SIV_{cpzant} (C-G on top of a U-A instead of the opposite). Covariances: YR265 has never been UG265; loop C of SIV_{cpzant}, HIV-1_{Ant70} (subtype O), and all subtype C HIV-1 viruses can form an internal base pair, thereby lengthening stem C by 1 bp and shortening loop C by 2 nt. Y, pyrimidine; R, purine; N, A, C, G, or U; O, N or nothing.

Plasmid constructions. Standard techniques were used for molecular cloning (65), and the nucleotide positions given are those of the HIV-1_{Lai} genomic RNA. Plasmid pSVC21.BH10, a gift of E. Cohen, encodes an infectious molecular clone derived from the IIIB strain of HIV-1 (18, 62). The plasmid also carries a simian virus 40 origin of replication for expression in COS cells, which are African green monkey kidney cells transformed by simian virus 40 (24). All the glassware used in this study was cooked overnight, and all the H_2O used for in vitro experiments was diethylpyrocarbonate treated.

The kissing-loop hairpin of pSVC21.BH10 was altered by cassette mutagenesis of plasmid pBH and transfer of the mutated region into pSVC21.BH10. To prepare pBH, pSVC21.BH10 was cleaved with *Bgl*II and *Apa*I to extract the 18-to-1556 region of the HIV-1 genome. The *Bgl*II-*Apa*I fragment (*Bgl*II side filled in) was then ligated into *Sac*I-*Apa*I-digested pBluescript KS$^-$ (38). This was followed by digestion with *Nar*I and *Bss*HII to create a gap between nt 187 and 261 (the *Bss*HII site had been blunt ended with mung bean nuclease). We then ligated two ~70-bp duplexes into the gap created by the *Nar*I and *Bss*HII digestions described above. One insert, ACS$^-$, contains a mismatch at the top of stem C (this shortens stem C by 1 bp and lengthens loop C by 2 nt) and has 3 mutations in loop C so that it is no longer autocomplementary (Fig. 1). The other insert, Δ248-261, is self-explanatory: the 5′ strand of stem C and most of loop C are deleted (Fig. 1). (Because the HIV-1 wild-type sequence has a GC at nt 247 and 248 and nt 261 and 262, the deletion also could have been named Δ247-260

TABLE 1. Comparison of HIV-1_{Lai} L-early *gag* sequences[a] with cognate sequences from HIV-1_{Ant70} (subtype O) and two SIV_{cpz} isolates (SIV_{cpzant} and an isolate from Gabon [SIV_{cpzgab}])

Hairpin or sequence	% Identity[b]				Rank
	HIV-1_{Ant70}	SIV_{cpzant}	SIV_{cpzgab}	Avg	
AUG[c]	85	77	96	86	1
KLD[c]	77	77	89	81	1
SD[c]	47	63	95	68	3
PBS-KLD linker[d]	77	63	60	67	3
Hairpin 3[c] + adjacent nt[e]	58	42	65	55	5
AU-rich interhairpin region[f]	44	44	67	52	5

[a] The L sequence extends from nt 200 to nt 335. The *gag* gene starts at nt 336. The nucleotide sequence conservation of the KLD and AUG hairpin within the HIV-1/SIV_{cpz} lineage appears to be higher than the amino acid sequence conservation of any HIV-1 protein within the HIV-1 family (68).

[b] With HIV-1_{Lai} sequence.

[c] Depicted in Fig. 1.

[d] The 200-to-242 region (Fig. 1).

[e] The 310-to-335 region (Fig. 1).

[f] The 301-to-309 region (Fig. 1).

or Δ249-262. However, the functional result is unchanged; stem C and the autocomplementary sequence are made inoperational through complete or quasicomplete destruction.) For duplex formation between the two ~70-nt complementary DNA oligonucleotides, 11 μg of each synthetic strand, dissolved in 20 μl of buffer TNE, was incubated for 10 min at 85°C in a G76 gyratory water bath (New Brunswick Scientific) covered with a glass plate; this was followed by shutting off water bath heating and letting the tube incubate overnight at slowly decreasing temperature. These duplexes were phosphorylated prior to ligation. The *Nar*I-*Spe*I fragments of pBHACS$^-$ and pBHΔ248-261 (i.e., the 187-to-1052 regions of the respective genomes) were then cloned into *Nar*I-*Spe*I-digested pSVC21.BH10 to yield eukaryotic expression vectors, pSVC21ACS$^-$ and pSVC21Δ248-261, respectively, containing full-length mutant HIV-1 proviral DNA. A third mutant plasmid, pSVC21Δ241-256, was prepared by PCR-based mutagenesis (46). (Because of a G at nt 241 and 257 in wild-type HIV-1, Δ241-256 also could have been named Δ242-257.) All constructs were sequenced to verify that the correct mutations had been achieved.

Transfections and virus preparation. Ten to 30 100- by 20-mm tissue culture dishes of COS-7 cells were transfected with plasmids pSVC21ACS$^-$ and pSVC21Δ248-261 (10 μg/dish) by the calcium phosphate method (33). In each transfection experiment, an equal number of tissue culture dishes was concurrently transfected with plasmid pSVC21.BH10 to produce the control BH10 virus to which mutants were compared. Viruses were isolated from the Dulbecco modified Eagle medium-fetal calf serum cell culture supernatant (7 ml/dish) at 63 h posttransfection. The supernatant was first centrifuged in a Beckman GS-6R rotor at 3,000 rpm for 30 min, and the viruses were then pelleted from this clarified COS-7 culture supernatant fluid by centrifugation in a Beckman Ti45 rotor at 35,000 rpm for 1 h at 4°C. Unless otherwise specified, the viral pellet was then purified by centrifugation at 26,500 rpm for 1 h at 4°C through 4 ml of 15% sucrose in buffer TNE onto a 2-ml 65% sucrose cushion in buffer TNE by using a Beckman SW41 rotor. The average virus yield was 4×10^8 virions per dish (assuming 2,000 capsid proteins per virion).

Infectivity assay. The numbers of 50% tissue culture infective doses ($TCID_{50}$) contained in mutant and wild-type viral preparations were measured in two 96-well flat-bottom plates as previously described (34). To perform each experiment in octuplicate, each of the eight wells in the second vertical row contained 12.8 μl of clarified COS-7 culture supernatant fluid in a final volume of 200 μl of R-20 medium containing 2×10^4 MT-4 target cells (a human T-cell line carrying human T-cell leukemia virus type 1 [28]). The 3rd to 11th vertical rows contained serial dilutions of the virus (from 4^{-1} to 4^{-9} dilutions). Culture fluids were replaced at day 4 after infection. The cytopathic effects (multinucleated giant cell formation-syncytium formation with ballooning cytoplasm) were assessed at days 4 and 7 after infection, and the number of $TCID_{50}$ was calculated by the method of Reed and Muench (16). One $TCID_{50}$ is the smallest amount of virus able to infect 50% of cell cultures at day 7, as measured by visible cytopathic effects. Each viral infectious titer is reported as the number of $TCID_{50}$/ng of capsid protein ± the standard error of the mean (SEM).

Physical virus titer. The physical virus titer was determined by estimating the amount of capsid protein (CAp24) in either purified viruses or clarified COS-7 culture supernatant fluid. Clarified COS-7 culture supernatant fluid (or a virus sample) was serially diluted (with the goal of obtaining at least one dilution containing 3 to 20 ng of capsid protein) and assayed by using a CAp24 enzyme-linked immunosorbent assay detection kit according to the manufacturer's (Abbott Laboratories) recommendations. The error for such measurements is 10%.

HIV-1 RNA isolation. Viruses were disrupted in 0.5 to 1 ml of sterile lysis buffer consisting of 50 mM Tris (pH 7.4), 10 mM EDTA, 1% sodium dodecyl sulfate (SDS), 50 mM NaCl, 50 μg of yeast tRNA per ml, and 100 μg of proteinase K per ml (20). Resuspended pellets were incubated at 37°C for 30 min and then extracted three times with an equal volume of buffer-saturated phenol-chloroform-isoamyl alcohol (25:24:1; pH 7.5). The aqueous phase, containing the viral RNA, was precipitated in 70% ethanol at −80°C with 0.3 M sodium acetate (pH 5.2). Viral RNA pelleted from the ethanol suspension was dissolved in a buffer containing 10 mM Tris (pH 7.5) and 1 mM EDTA.

Dot blot hybridization of RNA samples. The amount of genomic RNA in viral RNA samples was quantitated by hybridization (65) with radioactive antisense RNA 636-296, a 356-nt RNA that is antisense of the 296-to-636 region of the HIV-1 genome. This RNA was prepared by cutting plasmid pLJ230′ with *Rsa*I and transcribing it with SP6 RNA polymerase in the presence of [^{35}S]CTP or [^{32}P]CTP (39). Antisense RNA 636-296 had specific activities of $>10^8$ cpm/μg. A range of 5×10^6 to 1×10^9 copies of in vitro-transcribed HIV-1 RNA 230-790 (39) was used as the standard, from which the numbers of wild-type and mutant genomic HIV-1 RNAs were deduced. HIV-1 RNA samples were vacuum transferred to a Hybond N$^+$ nylon membrane (Amersham, Oakville, Canada) sandwiched within a Hybri-Dot filtration manifold (Bethesda Research Laboratories). After drying, cross-linking (0.12 J/cm^2 on a UV Stratalinker 2400 [Stratagene]), and prehybridization (in 6× SSPE [1× SSPE is 0.15 M NaCl, 10 mM NaH_2PO_4, and 1 mM EDTA {pH 7.4}]–50% formamide–10% dextran sulfate–1.5% SDS–5× Denhardt's reagent–0.01% salmon sperm DNA), the nylon membrane was hybridized overnight (in prehybridization buffer devoid of Denhardt's reagent at 42°C with shaking) to approximately 10^7 cpm of antisense RNA 636-296. This was followed by three washes (1× SSC [1× SSC is 0.15 M NaCl plus 0.015 M sodium citrate]–0.1% SDS at room temperature, 0.2× SSC–0.1% SDS at 35°C, and 0.2× SSC–0.1% SDS at 45°C) and autoradiography. The autoradiograms were scanned with an LKB Ultroscan XL laser densitometer, and to confirm the scans, the radioactivity present in each spot of the nylon membrane was also scintillation counted.

Electrophoretic and thermal analyses of HIV-1 genomic RNA. The dimeric nature of the encapsidated viral RNA was assessed by nondenaturing Northern (RNA) blot analysis (20, 35) of RNA samples dissolved in buffer L and run on 1% agarose gels in buffer TBE_2 at 4°C or room temperature (39). We found that running the gel at 70 V rather than our standard 95 to 100 V reduced the smearing to a level that allows conclusive interpretations. For thermal analysis, the RNAs were incubated at the indicated temperatures for 10 to 40 min prior to electrophoresis. After the RNA bands had been transferred from the agarose gel to a Hybond N$^+$ nylon membrane (Amersham), the nylon membrane was treated exactly as described above for the dot hybridization procedure.

Preparation and dimerization of in vitro-transcribed HIV-1 RNAs. Plasmids pBL (39), pBHACS$^-$, and pBHΔ248-261 were cleaved with *Acc*I and transcribed with T7 RNA polymerase to yield HIV-1 RNAs 1-508, 1-508ACS$^-$, and 1-508Δ248-261, respectively, all ending at G508 (39). The dimerization procedures, including attempts at preparing loose and tight dimers from the mutant transcripts, were described previously (39, 40).

Electrophoretic analysis of spliced and unspliced viral RNAs. Total cellular RNA extracted from COS-7 cells was purified with a commercial RNA extraction kit (Biotecs, Houston, Tex.). The extracted RNA was treated with 100 U of DNase I, followed by phenol-chloroform extraction and ethanol precipitation, to ensure the removal of any contaminating plasmids and cellular DNA. The RNA pellets were resuspended in diethylpyrocarbonate-treated double-distilled water. RNA samples (up to 20 μg) were fractionated on 1% agarose gels containing formaldehyde as denaturant (8). RNA molecules were transferred to a Hybond N$^+$ nylon membrane (Amersham) and hybridized by using pBH10 viral DNA as a radiolabelled probe (nick translation system; Life Technologies, Toronto, Canada) as previously described (8).

RESULTS

Near normal amounts of CAp24 produced after transfection of COS-7 cells by plasmids mutated in the kissing-loop hairpin. To produce HIV-1 viruses mutated within the KLD, COS-7 cells were transfected in parallel with equal amounts of control plasmid pSVC21.BH10 and mutant plasmids pSVC21ACS$^-$ and pSVC21Δ248-261. In pSVC21ACS$^-$, five point mutations were introduced in loop C in order to alter its sequence and render it nonautocomplementary (GAAGCGC GC262 was replaced by AGAUCACUC262) (Fig. 1). In pSVC21Δ248-261, the 5′ strand of stem C and most of loop C were deleted (Δ248-261; Fig. 1). The average amounts of ACS$^-$ and Δ248-261 viruses produced at 63 h posttransfection, as measured by the number of capsid proteins (CAp24) present in the culture supernatant and in the purified virus fraction, were 85 and (55 ± 15)%, respectively, of wild-type samples (not shown). This indicates that the mutations introduced had no major effect on HIV-1 genomic DNA transcription and virus production. This is supported by the results of recent experiments showing that the pSVC21Δ241-256 molecular clone produced 50% ± 5% less CAp24 than did the pSVC21.BH10 clone (46) (Fig. 1).

ACS$^-$ and Δ248-261 viruses are at least 99.25 and 99.96% less infectious, respectively, than are wild-type viruses. To assess the infectivity of the virus produced, the numbers of $TCID_{50}$ contained in two independent preparations of ACS$^-$ viruses and three independent preparations of Δ248-261 viruses were measured. Each experiment was performed in octuplicate (see Materials and Methods). Since each experiment involved serial dilutions, the results are best presented in logarithmic form (Table 2). Table 2 shows that the ACS$^-$ and Δ248-261 viruses contained 130 to 300 and 2,500 to 8,000 times fewer $TCID_{50}$ (per ng of capsid protein), respectively, than did the wild-type virus. As an independent verification, numerous CAp24 enzyme-linked immunosorbent assays were also performed with relevant viral dilutions to confirm that physical titers correlated with infectivity results (data not shown). Two possible causes of this low infectivity were investigated.

Mutant viruses display a 45 to 75% reduction in encapsidation efficiency. Viral genomic RNA was extracted from equiv-

TABLE 2. Infectious titers of wild-type viruses relative to those of mutant viruses[a]

Mutant	Infectivity test no.	Log BH10/mutant ratio	Overall avg
ACS$^-$	1	2.15 ± 0.2	2.3 ± 0.15
	2	2.4 ± 0.25	
Δ248-261	3	3.9 ± 0.25	3.65 ± 0.25
	4	3.2 ± 0.2	
	5	3.85 ± 0.3	

[a] In each infectivity test, the number of $TCID_{50}$ per nanogram of capsid protein (CAp24) was determined in octuplicate by using fourfold serial dilutions against a control BH10 population (see Materials and Methods). The data shown were determined by the method of Reed and Muench. The SEMs are also shown.

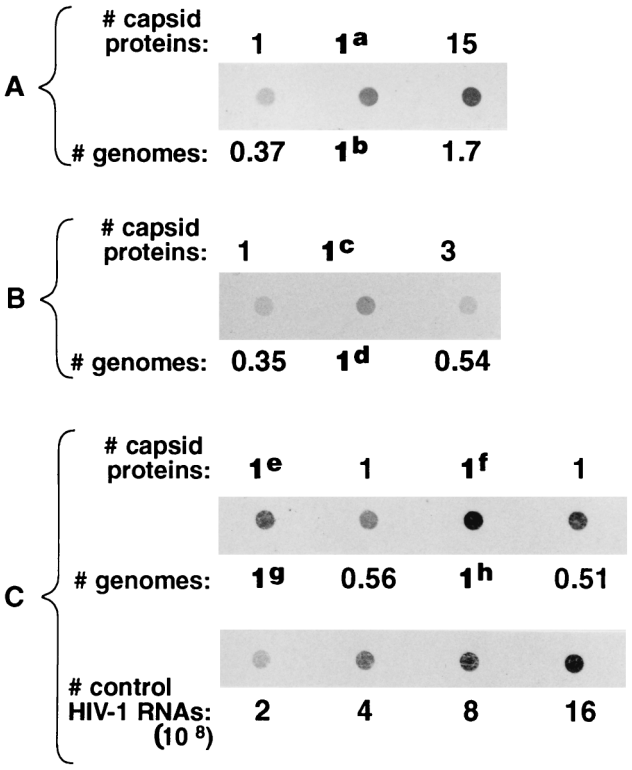

FIG. 3. Mutant genomic RNAs are poorly encapsidated. Hybridization of RNA dot blots with ^{35}S-labeled antisense RNA 636-296, a 356-nt probe that is antisense of the 296-to-636 region of the HIV-1 genome (see Materials and Methods). (A) Comparison of BH10 viral RNA from first transfection with ACS$^-$ viral RNA from first transfection. (B) Comparison of BH10 viral RNA from second transfection with ACS$^-$ viral RNA from second transfection. (C) Comparison of BH10 viral RNA from third and fourth transfections with Δ248-261 viral RNA from third and fourth transfections. All data are normalized relative to the numbers of capsid proteins (CAp24) and genomic RNAs in the control BH10 viruses. These values (1^a to 1^h) are 2.72×10^{10} CAp24, 8.8×10^7 genomic RNAs, 5.55×10^{11} CAp24, 10.3×10^7 genomic RNAs, 2.18×10^{11} CAp24, 8.7×10^8 genomic RNAs, 3.46×10^{11} CAp24, and 18.4×10^8 genomic RNAs, respectively. The control HIV-1 RNAs used to quantitate the amounts of genomic RNAs in the dot blot shown in panel C are also presented. The control HIV-1 RNA was RNA 230-790 obtained from the in vitro transcription of plasmid pLJ230 cut with *Dra*I (39). The number of viruses is expressed as the number (#) of capsid proteins (CAp24). Experiment B was done with viruses purified by pelleting in the absence of 15% sucrose and a 65% sucrose cushion (see Materials and Methods). The amount of CAp24 was measured as described in Materials and Methods. The amount of CAp24 per genome in wild-type virus varies with the method used to purify the virus.

alent amounts of virus, as determined by an antigen capture assay to detect CAp24 (see Materials and Methods). Virion RNA was then detected by dot blot hybridization analysis with a ^{35}S-labeled HIV-1 riboprobe (see Materials and Methods). The amount of HIV-1 RNA present in each spot was quantitated by scanning the resulting autoradiograms and by scintillation counting of the individual spots. Figures 3A and B show that the number of genomic RNAs per unit of capsid protein (± SEM) of the displayed ACS$^-$ viruses is 75% ± 6% lower than the number of genomic RNAs per unit of capsid protein of wild-type viruses. This value was independent of the method of virus purification (compare Fig. 3A and B). This encapsidation defect could have two explanations; the first is much more likely than the second. Either ACS$^-$ viruses packaged far fewer genomic RNAs per virion, or their capsid shells contained far more capsid proteins than normal. We do not distinguish between these two types of encapsidation deficiencies. Figure 3C shows that the number of genomic RNAs per unit of capsid protein (± SEM) of the displayed Δ248-261 virus is 46.5% ± 2.5% lower than that in the wild-type control. It is surprising that this physically more drastic mutation should have a smaller effect on encapsidation. Considering all our experimental results (seven dot blots for two independent ACS$^-$ preparations and five dot blots for three independent Δ248-261 preparations), the final numbers of genomic RNAs per unit of ACS$^-$ and Δ248-261 capsid protein were 23.5% ± 6% and 57% ± 3%, respectively, of wild-type levels. We conclude that mutations in the kissing-loop hairpin have moderate effects on HIV-1 genomic RNA encapsidation and that the precise strength of the effect may not be linearly related to the size of the mutation. This apparent nonlinearity would be easiest to rationalize if the KLD could interact with other regions of the HIV-1 genome, thereby more easily allowing for suppressor effects of some sequence changes.

Mutant viruses contain 33 to 50% less dimeric genomic RNA than do wild-type viruses. To investigate the effects of KLD alterations on the dimerization of HIV-1 genomic RNA, the isolated genomic RNAs were characterized by nondenaturing Northern analysis with a ^{35}S-labeled HIV-1 riboprobe. Figure 4a shows that barring what seems to be RNA aggregates near the top of the gel, there was one predominant HIV-1 RNA species in the wild-type viral RNA sample (lane 1; its size was that of a dimeric RNA) and two equally labeled species in the Δ248-261 RNA preparation (lane 5; their sizes corresponded to those of a monomeric RNA and a dimeric RNA). A scan of lanes 1 and 5 (that of lane 5 was translated toward the right for easier display) revealed that wild-type and Δ248-261 viral RNAs were ~85 and ~50% dimeric, respectively (Fig. 4b). In both wild-type and mutant samples, the dimeric RNA species dissociated at approximately 50°C (Fig. 4a, lanes 3 and 7) and then migrated like the lower band of the mutant RNA sample, which had the same mobility as denatured HIV-1 genomic RNA prepared by in vitro transcription (not shown). Together, the scans of Fig. 4 and the scans from Northern blots of two more independent preparations of Δ248-261 and BH10 viruses indicate that BH10 viral RNA was 1.75 (SEM, ±0.25) times more dimeric than was Δ248-261 viral RNA (not shown). Nondenaturing Northern analysis of ACS$^-$ HIV-1 RNAs also uncovered a lower percentage of dimeric RNAs than that in BH10 viral RNA samples, but because all ACS$^-$ viral RNA samples were more smeared as a result of having been electrophoresed at 90 V (see Materials and Methods), we cannot regard the ACS$^-$ data as quantitative (data not shown).

Near normal splicing of viral RNA from Δ241-256 viruses. The fact that the ACS$^-$, Δ248-261, and Δ241-256 mutations did not strongly affect virus production suggests that none of these mutations abrogated DNA transcription from the up-

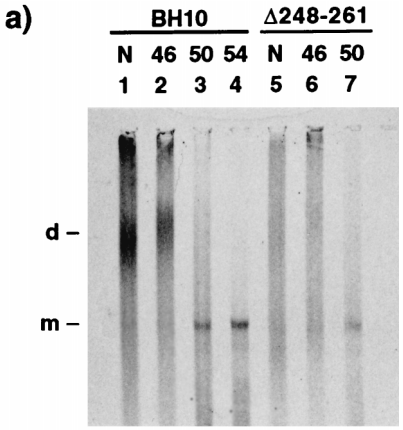

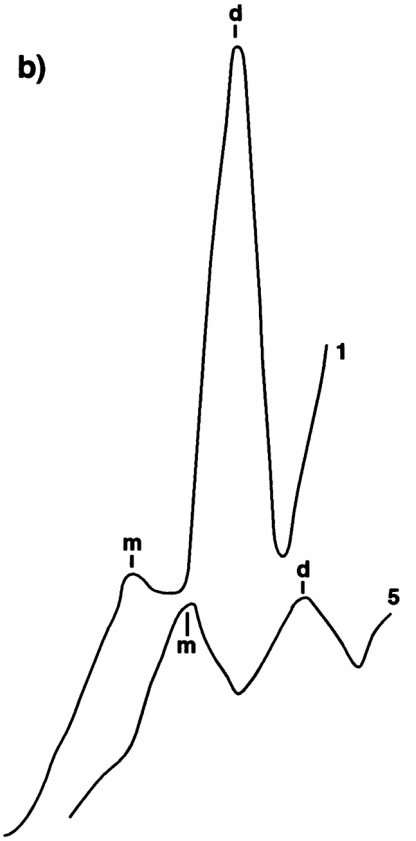

FIG. 4. (a) Dimerization level and thermal stability of the viral RNA isolated from equal amounts of BH10 and Δ248-261 HIV-1 viruses (as measured by the number of capsid proteins). BH10 viral RNAs (3.7×10^9) and Δ248-261 viral RNAs (1.9×10^9) (in a volume of 2 μl) were dissolved in a mixture of 6 μl of water–2 μl of 5× concentrated buffer L. N (for native) samples were left on ice for 10 min. The other samples were incubated in buffer L at the temperatures indicated (°C) for 10 min. After incubation, all samples were loaded without delay and with the voltage on. After electrophoresis (70 V, 4 h, 1% agarose in buffer TBE_2 at room temperature), the samples were Northern blotted, hybridized, and autoradiographed. d, dimeric RNA; m, monomer. Monomeric and dimeric positions were confirmed with a full-length HIV-1 genome prepared by in vitro transcription (41). The autoradiogram was exposed for 4 days. (b) Scans of lanes 1 and 5 from panel a. For easy display, the scan of lane 5 was displaced toward the right, relative to the scan of lane 1.

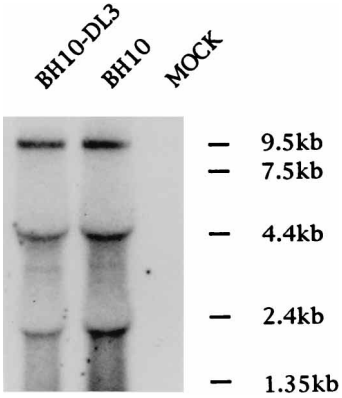

FIG. 5. Mutant intracellular viral RNA is spliced at near normal levels. Cellular RNA was extracted from COS-7 cells after transfection with plasmid pSVC21.BH10 (BH10) or pSVC21Δ241-256 (BH10-DL3). After electrophoresis on a denaturing gel (see Materials and Methods), the samples were Northern blotted, hybridized, and autoradiographed. MOCK, mock infected.

stream long terminal repeat promoter, splicing from the downstream 5′ splice junction, or RNA translation from the further downstream AUG initiation codon of the *gag* gene. Near normal expression of CAp24 seemingly requires near normal expression and cytoplasmic accumulation of full-length viral RNA, which itself requires near normal expression of Tat and Rev, which are themselves translated from spliced mRNAs. Reverse transcription (RT)-PCR assays performed with total cellular RNA extracted from COS-7 cells transfected with pSVC21.BH10 or pSVC21Δ241-256 and designed to assay for all viral RNA made (spliced and unspliced) have shown that the mutant plasmid produced about half the amount of RNA produced by the control plasmid (46). In addition, chloramphenicol acetyltransferase (CAT) assays (performed after replacing the sequences downstream of nt 285 with a CAT gene to yield plasmids Δ241-256-CAT and BH10-CAT) have shown the amount of CAT produced per mutant plasmid to be 55% ± 7% lower than control values (46). The consistency among the CAp24, CAT, and RT-PCR results suggests that the reduction in CAp24 production has only one cause, namely, a transcription efficiency reduced by half, and that splicing and translation should be hardly affected by the Δ241-256 mutation. This is confirmed in Fig. 5, which shows, together with the scans of the autoradiogram (not shown), that the total amount of cytoplasmic viral RNA produced by plasmid pSVC21Δ241-256 was reduced, consistent with the transcriptional defect already demonstrated (46), and that the proportion of spliced RNAs appeared to be reduced by an insignificant 25% in the mutant virus.

ACS^- and Δ248-261 RNAs prepared by in vitro transcription do not dimerize. $HIV\text{-}1_{Lai}$ RNA transcripts containing the first 500 to 1,000 nt of the HIV-1 genome can form two types of dimers, loose and tight dimers (39, 40, 52). Loose dimers are formed by incubating HIV-1 RNA transcripts containing the KLD in low- or high-ionic-strength buffer (buffer H) at 0 to 37°C. Tight dimers are formed by incubating the transcripts at 55 to 60°C in low-ionic-strength buffer L. Figure 6 shows that RNAs extending to G508 and containing the ACS^- or Δ248-261 mutation (lanes 2, 3, 8, and 9) do not form loose dimers under low- and high-ionic-strength conditions. These RNAs cannot form tight dimers either (Fig. 6, lanes 1 and 10). Bear in mind that the RNA transcripts of Fig. 6 were studied at a 1,000-fold-higher concentration than were the genomic RNAs of Fig. 4. The background amount of dimer (<10%) (Fig. 6,

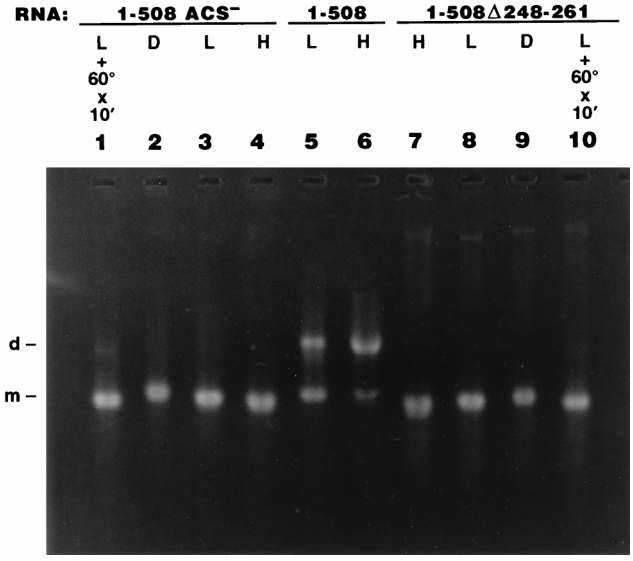

FIG. 6. HIV-1 RNAs mutated in the KLD and ending at G508 do not dimerize. RNA (500 ng) was electrophoresed (10 V/cm, 70 min) at room temperature on a 2.5% agarose gel containing buffer TBM. L, low-salt conditions, i.e., incubation at 0°C for 30 min in buffer L; H, incubation at 37°C for 30 min in buffer H; D, denatured sample; L + 60° × 10′, low-salt conditions followed by heating at 60°C for 10 min. d, dimeric RNA; m, monomer.

lanes 1 and 10) has no biological significance. Incubations at 50 to 60°C in buffer L or at 60 to 70°C in buffer H of control RNAs containing no obvious autocomplementary sequences often give rise to such background formation of dimers (reference 39 and unpublished data). This is probably due to some stem-loops having a melting temperature close to the incubation temperature and occasionally switching from intrastrand to interstrand hydrogen bonding. This artifactual dimerization always results in the formation of between 0 and 10% dimer (see Fig. 4 in reference 39). Incubations at 46, 49, 52, 55, 58, and 65°C for 10 to 40 min never favored the formation of more than 10% dimeric 1-508ACS$^-$ and 1-508Δ248-261 RNAs (not shown), in accordance with the idea that this low level of dimerization is of artifactual origin and that no hidden meaning should be attached to it. Together, the in vitro data and in vivo results suggest that a dimerization signal exists downstream of G508, i.e., downstream of the KLD and 3′ DLS (the 3′ DLS is a dimerization signal located within the early *gag* coding sequence of HIV-1_{Mal} [39, 40, 57]), but that the rate of dimerization is controlled by the kissing-loop hairpin.

DISCUSSION

Pleiotropic effects of the kissing-loop hairpin on HIV-1 physiology or underestimation of the RNA dimerization and packaging defect? Under the most favorable theoretical scenario—monomeric genomic RNAs being encapsidated into HIV-1 as efficiently as dimeric genomic RNAs (highly debatable), viruses containing only one genomic RNA being totally avirulent (highly unlikely), and the lower dimerization level being unrelated to the lower encapsidation levels (questionable)—simple statistics show that if our encapsidation and dimerization results are taken at face value, they can account for only ~0.4% of the infectivity lost by the Δ248-261 viruses and 25% of the infectivity lost by the ACS$^-$ viruses. (It should be recognized at the outset that such a scenario is impossibly unrealistic; if the first assumption is true, the third one cannot be, and mutatis mutandis, because viruses having encapsidated one genomic RNA are bound to contain a monomeric genome and appear to be dimerization deficient if only by default.) We can imagine the following two nontrivial explanations for this apparent paradox between moderate effects of the mutations on HIV-1 formation in the cytoplasm of COS cells and massive effects on the infection of MT-4 cells: the 248-to-261 region has highly pleiotropic effects on HIV-1 physiology or the dimerization and encapsidation data should not be extrapolated from transfected cells to cells infected by one virus.

Because the kissing-loop hairpin is located within 30 to 80 nt of the 5′ splice junction, the primer binding site, the 5′ long terminal repeat domain, and the AUG codon of the *gag* gene, it might influence RNA splicing, minus-strand DNA synthesis, viral DNA transcription, or p55^{gag} synthesis. We think that RNA or DNA sequences corresponding to the kissing-loop hairpin might stimulate viral DNA transcription by a factor of almost 2, but we doubt that the kissing-loop hairpin significantly influences RNA splicing, RNA translation, or minus-strand DNA synthesis for the following reasons. (i) The transfected ACS$^-$ molecular clone produced as much CAp24 as did the control BH10 clone; the transfected pSVC21Δ248-261 and Δ241-256 plasmids produced 45 and (50 ± 5)% less CAp24, respectively, than did the control BH10 plasmid (see Results), consistent with a negligible to moderate transcription deficiency in these three mutants. (ii) The reduced CAp24 yield from plasmid pSCV21Δ241-256 is fully explained by its reduced transcriptional potential (see Results). (iii) The transfected pSVC21Δ241-256 plasmid was not significantly deficient in splicing (Fig. 5) and displayed an ability for minus-strand viral DNA synthesis that was at least as good as normal (45). (iv) It is unlikely that a 25% reduction in splicing (consistent with Fig. 5) could reduce the relative numbers of Env, Tat, Rev, and other "accessory" proteins so much as to cause a dramatic effect on infectivity. Otherwise, the putative Tat protein shortage would have resulted in a lower CAp24 production than what was predicted by the CAT and RT-PCR assays (see Results), and the lower concentration of Rev proteins should have increased transfer time from nucleolus to cytoplasm, probably reducing CAp24 production. Consistent with the above, we have found that the Δ241-256 mutation does not reduce the half-life of viral genomic RNA within COS-7 cells (46). Lastly, we have not ruled out the odd possibility that RNA recombination (22, 23, 50), plus-strand DNA initiation, and/or second-strand transfer might be affected by our mutations; we simply note that considerable mutations within loop C had no effect on plus-strand DNA initiation and/or second-strand transfer and that the deletion of the whole kissing-loop hairpin had only a moderate (66%) effect (56) (Table 3), i.e., nothing sufficient, even after compounding with the effects of our mutations on viral RNA synthesis, splicing, dimerization, and encapsidation, to explain the low infectivities of our mutants. We assume that the transcription and splicing defects of the pSVC21Δ248-261 plasmid are similar to or, if anything, slightly smaller than those of the pSVC21Δ241-256 plasmid. This is based on (i) their identical efficiency at producing CAp24, (ii) the fact that the Δ241-256 mutation destroys more than the kissing-loop hairpin (it also destroys the short stem on which it is seated [Fig. 1]), and (iii) the fact that they produce viruses which are equally noninfectious (see Results) (45).

A solution to the paradox. Faced with a dearth of simple explanations, we propose that a substantial, if not the main, cause of the low infectivities of our mutant HIV-1 viruses remains their RNA dimerization and encapsidation defects, i.e., our assays have underscored the actual level of viral RNA dimerization and encapsidation within an MT-4 cell infected by one HIV virus. Three elements are key to our reasoning. (i)

TABLE 3. Effects of mutations within the KLD on various processes

Mutation or location of mutated nucleotides	Effect on[a]:								Reference
	Infectivity	RNA encapsidation	Genomic RNA dimerization	Splicing	CAp24 produced after transfection	Viral RNA transcription	Minus-strand DNA synthesis	Plus-strand DNA initiation and/or second template transfer	
Δ248-261	++++	+	+	ND	+	ND	ND	ND	This study
Δ241-256	++++	ND	ND	−	+	+	−	ND	This study
Five point mutations in 254-261	+++	+	+?	ND	−	ND	ND	ND	This study
241-253 linker substitution	Delayed	++[b]	ND	−	−	ND	ND	ND	36
Three point mutations in 248-251	ND	±	ND	ND	−	ND	ND	ND	49
Three point mutations in 257-259	++	+[c]	+	ND	ND	ND	ND	ND	27
Δ259-262	++[d]	+	−	ND	−	ND	−	ND	6
Δ248-270	++++	+[e]	ND	ND	−	ND	ND	+	56
Three point mutations in 257-259	++	+	ND	ND	−	ND	ND	−	56
255-263 linker substitution	+++	+	ND	ND	−	ND	ND	−	56

[a] −, no significant reduction (in most studies, no significant reduction could not exclude a 10 to 40% reduction); ±, 10 to 40% reduction; +, 40 to 80% reduction; ++, 80 to 98% reduction; +++, 98 to 99.8% reduction; ++++, >99.8% reduction; ND, not done.
[b] 78 to 85% reduction in encapsidation.
[c] Data not originally quantitated.
[d] Approximate 10-fold reduction in infectivity.
[e] Fivefold reduction.

In vitro RNA dimerization studies have always pointed out that the RNA concentration is a critical parameter for promoting HIV-1 RNA dimerization (40, 41, 48, 58). (ii) Among the processes of RNA synthesis, splicing, translation, dimerization, and encapsidation, the first three are unlikely to be affected by viral RNA concentration (because they rely on interactions with cellular components) and the fourth and fifth are likely to be affected (because they rely on interactions between viral components). Genomic RNA encapsidation might be concentration dependent to the extent that the KLD might be an encapsidation signal or to the extent that genomic RNA encapsidation might be stimulated by genomic RNA dimerization. (iii) The number of RNA genomes per infected cell is particularly high in massively infected or transfected cell cultures because of the high multiplicity of infection or the high level of transfected DNA per competent cell (15); in contrast, the purpose of a $TCID_{50}$ assay is to identify the lowest virus concentration able to yield cytopathic effects in, e.g., MT-4 cells, one cytopathic effect (plaque formation) usually being the product, with wild-type viruses, of one infectious viral particle (28). Plaque formation would require relatively massive excesses of our mutant viruses for either of the following reasons: to produce one (or a few) MT-4 cell(s) simultaneously hit by many mutant viruses to yield an intracellular genomic RNA concentration high enough to bypass the RNA dimerization defect (by virtue of the law of mass action) or to produce a massive number of infected MT-4 cells from which one or a few will, through some stochastic effect, lead to plaque formation. In other words, a moderate reduction in the percentage of dimeric RNA or its encapsidation level under the high intracellular viral RNA concentrations of a transfected cell might become a >99% average reduction under the (more physiological) conditions of one MT-4 cell being infected by one mutant virus; to achieve a cytopathic effect in one cell, either intracellular mutant viral RNA concentrations must reach levels similar to those found in transfected cells (achieved only when one cell is simultaneously infected by a large number of viruses) or, possibly, a large number of cells must adsorb viruses to increase the chance of stochastic effects which might cause rare plaque formations. Either mechanism yields small numbers of $TCID_{50}$ per unit of mutant virus. Unfortunately, the study of genomic RNA dimerization and encapsidation processes under conditions where mutant HIV-1 viruses are made to infect a normal cellular target at low multiplicities of infection is prohibitively expensive because not enough virus is produced to perform biochemical RNA analysis.

The kissing-loop hairpin: one element of a multipartite dimerization and encapsidation signal. Important purposes of the selective encapsidation process are (i) to concentrate RNA molecules within a small volume (the viral capsid) and (ii) to alter the composition of the packaged RNA so that it is no longer <1% HIV-1 RNA, as in the cytoplasm (17, 60), but is >50% HIV-1 RNA. This requires a ≥100-fold increase in packaging selectivity. The $Pr55^{gag}$ polyprotein offers such selectivity (25), but the HIV-1 RNA sequences involved in the necessary RNA-protein interactions are imperfectly known. No matter what the real contribution of the KLD to the encapsidation process is, it is easy to imagine how the KLD, together with the other encapsidation sites so far identified in the U5 region (70), near hairpin 3 (Fig. 1) (1, 11, 30, 44, 49), near the initiation codon of the *gag* gene (47), and further downstream (9), could achieve a 100-fold increase in encapsidation specificity or efficiency. One obvious implication of our results and those of our predecessors is that the encapsidation signal of HIV-1 is multipartite (see also references 7 and 49).

Genomic RNA dimerization and encapsidation: linked operations? The behavior of genomic RNA isolated from our kissing-loop-defective HIV-1 viruses is partially reminiscent of genomic RNA isolated from protease-deficient virions (20). First, genomic RNAs from both protease- and kissing-loop-defective virions are dimerization deficient (20) (this study). Second, we note that as in protease-deficient mutants, the electrophoretic distance between monomeric and dimeric Δ248-261 genomic RNAs in each RNA blot was longer (10% longer on average) than the corresponding distance in wild-type genomic RNA (Fig. 4b and data not shown), as if mutant

dimeric genomic RNA has a less compact structure (due to the putative inactivation of one of the wild-type interstrand linkages?). However, contrary to genomic RNA from protease-deficient mutants, Δ248-261 genomic RNA had a wild-type dissociation temperature (T_d), 48 to 50°C versus 48 to 53°C for wild-type samples (Fig. 4a and data not shown).

How can Δ248-261 HIV-1 genomic RNA appear to be dimerization deficient yet as stable as the wild type? At least two equally valid explanations can be offered. (i) Perhaps mutant viruses appear to be dimerization deficient only by default, having often encapsidated one single genomic RNA as a result of their encapsidation defect (this model must assume that genomic RNAs are usually monomeric at the time of encapsidation or that monomeric genomic RNAs are encapsidated as efficiently as are dimeric genomic RNAs). (ii) Perhaps the KLD controls dimerization initiation, but another locus determines the ultimate dimer stability; therefore, genomic RNA is slow to dimerize in the absence of an intact KLD. If wild-type genomic RNAs dimerize mostly within the virion, then one can imagine that the mutant genomic RNAs did not have the time to fully dimerize by the time they were harvested. If at the moment of encapsidation a significant proportion of wild-type genomic RNAs are dimeric while a significant proportion of KLD-deficient genomic RNAs are monomeric, one may further imagine that Pr55^{gag} polyprotein preferentially recognizes a structural motif present only in dimeric RNAs, in addition to incidentally exerting a twofold selectivity toward dimeric genomic RNAs by a variant of the law of mass action (whenever Pr55^{gag} catches one genomic RNA that happens to be linked to another one, it effectively catches two genomic RNAs in a single sweep). In this way, a dimerization defect causes an encapsidation defect.

Our results and the previous paragraph essentially point out that from a theoretical as well as an experimental point of view, genome dimerization and encapsidation appear to some extent coupled, with low encapsidation potentially leading to a deficit in the proportion of dimeric RNAs and low rates of dimerization potentially leading to low encapsidation. Therefore, the KLD could play a role in the encapsidation process without being a Pr55^{gag} polyprotein recognition site and an encapsidation signal in U5, near hairpin 3 or in the *gag* coding sequence, could reduce the proportion of dimeric RNAs in the isolated virions without being a site for interstrand linkages.

Having suggested above that the rate of genomic RNA dimerization is determined foremost by the KLD and secondarily by a postulated 3′ dimerization signal, we further propose that this 3′ dimerization signal is located downstream of the KLD and 3′ DLS. This would explain why genomic RNAs deprived of a correct KLD can dimerize and why short in vitro transcripts possessing an intact 3′ DLS but no KLD cannot dimerize (Fig. 6) (40). In this respect, we have recently discovered within the 3′ half of HIV-1 genomic RNA a 1,000-nt-long dimeric RNA region that has a T_d of 49°C (41).

Brief comparison with other studies. Relevant papers have been published after the present experiments were nearly completed (27, 49), after several drafts of this paper had been written (6), and after submission of the manuscript (56). Two of them (6, 27) studied (at least in a qualitative way) the effects of KLD mutations on viral infectivity, as well as genomic RNA encapsidation and dimerization. A third (56) studied two of the three parameters. Despite the numerous differences in virtually all of the experimental details (HIV-1 strains, target cells, mutations, transfection methods, infectivity assays, and degree of quantitation of the results) and several quantitative differences in the results, Table 3 shows that some harmony can be found between these various studies of the effects of mutations altering the kissing-loop hairpin (6, 27, 36, 49, 56) (this study). This is not the place to discuss in detail the quantitative differences between individual results. Among the scenarios described above, one implies that in the presence of a defective kissing-loop hairpin, in vivo dimerization occurs at a sufficiently slow rate and/or with a sufficiently low association constant that depending on the transfection or infection protocol, there is room for isolated viral RNAs to range from almost monomeric (e.g., in budding viruses from infected cells) to entirely dimeric (e.g., in late harvest viruses from transfected cells).

Conclusions. (i) The kissing-loop hairpin plays a role in genomic RNA dimerization and encapsidation and has dramatic effects on viral infectivity; it may play a modest role in viral RNA synthesis but does not seem to play a role in RNA splicing or translation. (ii) The kissing-loop hairpin could be profitably targeted by antisense constructs within an AIDS therapeutic program. (iii) The region of the dimeric HIV-1 genomic RNA which determines its T_d is not that which determines the rate of dimerization. It is tempting to speculate that in accord with the kissing-loop model of HIV-1 RNA dimerization, the kissing-loop hairpin controls the rate of dimerization of HIV-1 genomic RNA. (iv) The encapsidation and dimerization processes are to some extent coupled. The effect of the kissing-loop hairpin on one of these two processes could be an indirect one; the cause of this indirect effect would, however, be the direct involvement of the kissing-loop hairpin in the other process. (v) It is not excluded that a substantial cause of the lack of infectivity of HIV-1 viruses mutated in the kissing-loop hairpin is the dimerization and encapsidation defect shown here because of the respective differences in physiology between transfected and infected cells.

ACKNOWLEDGMENTS

This work was supported by a grant from the Medical Research Council of Canada to M.L.

We thank Rhona Rosenzweig for the preparation of the typed text.

REFERENCES

1. **Aldovini, A., and R. A. Young.** 1990. Mutations of RNA and protein sequences involved in human immunodeficiency virus type 1 packaging result in production of noninfectious virus. J. Virol. **64:**1920–1926.
2. **Baudin, F., R. Marquet, C. Isel, J.-L. Darlix, B. Ehresmann, and C. Ehresmann.** 1993. Functional sites in the 5′ region of human immunodeficiency virus type 1 RNA form defined structural domains. J. Mol. Biol. **229:**382–397.
3. **Bender, W., and N. Davidson.** 1976. Mapping of poly(A) sequences in the electron microscope reveals unusual structure of type C oncornavirus RNA molecules. Cell **7:**595–607.
4. **Bender, W., Y.-H. Chien, S. Chattopadhyay, P. K. Vogt, M. B. Gardner, and N. Davidson.** 1978. High-molecular-weight RNAs of AKR, NZB, and wild mouse viruses and avian reticuloendotheliosis virus all have similar dimer structures. J. Virol. **25:**888–896.
5. **Berkhout, B.** 1996. Structure and function of the human immunodeficiency virus leader RNA. Prog. Nucleic Acid Res. Mol. Biol. **54:**1–34.
6. **Berkhout, B., and J. L. B. Van Wamel.** 1996. Role of the DIS hairpin in replication of human immunodeficiency virus type 1. J. Virol. **70:**6723–6732.
7. **Berkowitz, R. D., M.-L. Hammarskjold, C. Helga-Maria, D. Rekosh, and S. P. Goff.** 1995. 5′ regions of HIV-1 RNAs are not sufficient for encapsidation: implications for the HIV-1 packaging signal. Virology **212:**718–723.
8. **Boulerice, F., S. Bour, R. Geleziunas, A. Lvovich, and M. A. Wainberg.** 1990. High frequency of isolation of defective human immunodeficiency virus type 1 and heterogeneity of viral gene expression in clones of infected U937 cells. J. Virol. **64:**1745–1755.
9. **Buchschacher, G. L., and A. T. Panganiban.** 1992. Human immunodeficiency virus vectors for inducible expression of foreign genes. J. Virol. **66:**2731–2739.
10. **Carr, J. K., M. O. Salminen, C. Koch, D. Gotte, A. W. Artenstein, P. A. Hegerich, D. St. Louis, D. S. Burke, and F. E. McCutchan.** 1996. Full-length sequence and mosaic structure of a human immunodeficiency virus type 1 isolate from Thailand. J. Virol. **70:**5935–5943.
11. **Clavel, F., and J. M. Orenstein.** 1990. A mutant of human immunodeficiency

virus with reduced RNA packaging and abnormal particle morphology. J. Virol. **64:**5230–5234.
12. **Clever, J., C. Sassetti, and T. G. Parslow.** 1995. RNA secondary structure and binding sites for *gag* gene products in the 5′ packaging signal of human immunodeficiency virus type 1. J. Virol. **69:**2101–2109.
13. **Clever, J. L., M. L. Wong, and T. G. Parslow.** 1996. Requirements for kissing-loop-mediated dimerization of human immunodeficiency virus RNA. J. Virol. **70:**5902–5908.
14. **Coffin, J.** 1984. Structure of the retroviral genome, p. 261–368. *In* R. Weiss, N. Teich, H. Varmus, and J. Coffin (ed.), RNA tumor viruses. Cold Spring Harbor Laboratory Press, Cold Spring Harbor, N.Y.
15. **Cullen, B. R.** 1987. Use of eukaryotic expression technology in the functional analysis of cloned genes. Methods Enzymol. **152:**684–703.
16. **Dulbecco, R.** 1988. The nature of viruses, p. 1–25. *In* R. Dulbecco and H. S. Ginsberg (ed.), Virology, 2nd ed. J. P. Lippincott, Philadelphia, Pa.
17. **Fan, H., and D. Baltimore.** 1973. RNA metabolism of murine leukemia virus: detection of virus-specific RNA sequences in infected and uninfected cells and identification of virus-specific messenger RNA. J. Mol. Biol. **80:**93–117.
18. **Fischer, A. G., E. Collalti, L. Ratner, R. C. Gallo, and F. Wong-Staal.** 1985. A molecular clone of HTLV-III with biological activity. Nature **316:**262–265.
19. **Fossé, P., N. Motté, A. Roumier, C. Gabus, D. Muriaux, J.-L. Darlix, and J. Paoletti.** 1996. A short autocomplementary sequence plays an essential role in avian sarcoma leukosis virus RNA dimerization. Biochemistry **35:**16601–16609.
20. **Fu, W., R. J. Gorelick, and A. Rein.** 1994. Characterization of human immunodeficiency virus type 1 dimeric RNA from wild-type and protease-defective virions. J. Virol. **68:**5013–5018.
21. **Gao, F., D. L. Robertson, S. G. Morrison, H. Hui, S. Craig, J. Decker, P. N. Fultz, M. Girard, G. M. Shaw, B. H. Hahn, and P. M. Sharp.** 1996. The heterosexual human immunodeficiency virus type 1 epidemic in Thailand is caused by an intersubtype (A/E) recombinant of African origin. J. Virol. **70:**7013–7029.
22. **Girard, P.-M., B. Bonnet-Mathonière, D. Muriaux, and J. Paoletti.** 1995. A short autocomplementary sequence in the 5′ leader region is responsible for dimerization of MoMuLV genomic RNA. Biochemistry **34:**9785–9794.
23. **Girard, P.-M., H. de Rocquigny, B.-P. Roques, and J. Paoletti.** 1996. A model of PSI dimerization: destabilization of the C^{278}-G^{303} stem-loop by the nucleocapsid protein (NCp10) of MoMuLV. Biochemistry **35:**8705–8714.
24. **Gluzman, Y.** 1981. SV40-transformed simian cells support the replication of early SV40 mutants. Cell **23:**175–182.
25. **Gorelick, R. J., S. M. Nigida, Jr., J. W. Bess, Jr., L. O. Arthur, L. E. Henderson, and A. Rein.** 1990. Noninfectious human immunodeficiency virus type 1 mutants deficient in genomic RNA. J. Virol. **64:**3207–3211.
26. **Guillon, C., F. Bedin, A. M. Fouchier, H. Schuitemaker, and R. A. Gruters.** 1995. Completion of nucleotide sequences of non-syncytium-inducing and syncytium-inducing HIV type 1 variants isolated from the same patient. AIDS Res. Hum. Retroviruses **11:**1537–1538.
27. **Haddrick, M., A. L. Lear, A. J. Cann, and S. Heaphy.** 1996. Evidence that a kissing loop structure facilitates genomic RNA dimerization in HIV-1. J. Mol. Biol. **259:**58–68.
28. **Harada, S., Y. Koyanagi, and N. Yamamoto.** 1985. Infection of HTLV-III/LAV in HTLV-I-carrying cells MT-2 and MT-4 and application in a plaque assay. Science **229:**563–566.
29. **Harrison, G. P., and A. M. L. Lever.** 1992. The human immunodeficiency virus type 1 packaging signal and major splice donor region have a conserved stable secondary structure. J. Virol. **66:**4144–4153.
30. **Hayashi, T., T. Shioda, Y. Iwakura, and H. Shibuta.** 1992. RNA packaging signal of human immunodeficiency virus type 1. Virology **188:**590–599.
31. **Hayashi, T., Y. Ueno, and T. Okamoto.** 1993. Elucidation of a conserved RNA stem-loop structure in the packaging signal of human immunodeficiency virus type 1. FEBS Lett. **327:**213–218.
32. **Huet, T., M.-C. Dazza, F. Brun-Vézinet, G. E. Roelants, and S. Wain-Hobson.** 1989. A highly defective HIV-1 strain isolated from a healthy Gabonese individual presenting an atypical Western blot. AIDS **3:**707–715.
33. **Jiang, M., J. Mak, M. A. Wainberg, M. A. Parniak, E. Cohen, and L. Kleiman.** 1992. Variable tRNA content in HIV-1_{IIIB}. Biochem. Biophys. Res. Commun. **185:**1005–1015.
34. **Johnson, V. A., and R. E. Byington.** 1990. Quantitative assays for virus infectivity, p. 71–86. *In* A. Aldovini and B. D. Walker (ed.), Techniques in HIV research. Stockton Press, New York, N.Y.
35. **Khandjian, E. W., and C. Méric.** 1986. A procedure for Northern blot analysis of native RNA. Anal. Biochem. **159:**227–232.
36. **Kim, H.-J., K. Lee, and J. J. O'Rear.** 1994. A short sequence upstream of the 5′ major splice site is important for encapsidation of HIV-1 genomic RNA. Virology **198:**336–340.
37. **Kung, H.-J., S. Hu, W. Bender, J. M. Bailey, N. Davidson, M. O. Nicolson, and R. M. McAllister.** 1976. RD-114, baboon, and woolly monkey viral RNAs compared in size and structure. Cell **7:**609–620.
38. **Laughrea, M., and L. Jetté.** 1994. A 19-nucleotide sequence upstream of the 5′ major splice donor is part of the dimerization domain of human immunodeficiency virus 1 genomic RNA. Biochemistry **33:**13464–13474.
39. **Laughrea, M., and L. Jetté.** 1996. Kissing-loop model of HIV-1 genome dimerization: HIV-1 RNAs can assume alternative dimeric forms, and all sequences upstream or downstream of hairpin 248-271 are dispensable for dimer formation. Biochemistry **35:**1589–1598.
40. **Laughrea, M., and L. Jetté.** 1996. HIV-1 genome dimerization: formation kinetics and thermal stability of dimeric HIV-1_{Lai} RNAs are not improved by the 1-232 and 296-790 regions flanking the kissing-loop domain. Biochemistry **35:**9366–9374.
41. **Laughrea, M., and L. Jetté.** Unpublished data.
42. **Laughrea, M., and P. B. Moore.** 1977. Physical properties of ribosomal protein S1 and its interaction with the 30S ribosomal subunit of *Escherichia coli*. J. Mol. Biol. **112:**399–421.
43. **Learn, G. H., B. T. M. Korber, B. Foley, B. H. Hahn, S. M. Wolinsky, and J. I. Mullins.** 1996. Maintaining the integrity of human immunodeficiency virus sequence databases. J. Virol. **70:**5720–5730.
44. **Lever, A., H. Gottlinger, W. Haseltine, and J. Sodroski.** 1989. Identification of a sequence required for efficient packaging of human immunodeficiency virus type 1 RNA into virions. J. Virol. **63:**4085–4087.
45. **Li, X., C. Liang, Y. Quan, M. A. Parniak, L. Kleiman, and M. A. Wainberg.** Identification of sequences downstream of the primer binding site that are essential for replication of the human immunodeficiency virus type 1. Submitted for publication.
46. **Liang, C., X. Li, M. A. Parniak, L. Kleiman, M. Laughrea, and M. A. Wainberg.** Unpublished data.
47. **Luban, J., and S. P. Goff.** 1994. Mutational analysis of *cis*-acting packaging signals in human immunodeficiency virus type 1 RNA. J. Virol. **68:**3784–3793.
48. **Marquet, R., F. Baudin, C. Gabus, J.-C. Darlix, M. Mougel, C. Ehresmann, and B. Ehresmann.** 1991. Dimerization of human immunodeficiency virus (type 1) RNA: stimulation by cations and possible mechanism. Nucleic Acids Res. **19:**2349–2357.
49. **McBride, M. S., and A. T. Panganiban.** 1996. The human immunodeficiency virus type 1 encapsidation site is a multipartite RNA element composed of functional hairpin structures. J. Virol. **70:**2963–2973.
50. **Mikkelsen, J. G., A. H. Lund, K. D. Kristensen, M. Duch, M. S. Sorensen, P. Jorgensen, and F. S. Pedersen.** 1996. A preferred region for recombinational patch repair in the 5′ untranslated region of primer binding site-impaired murine leukemia virus vectors. J. Virol. **70:**1439–1447.
51. **Muriaux, D., H. De Rocquiquy, B.-P. Roques, and J. Paoletti.** 1996. NCp7 activates HIV-I_{Lai} RNA dimerization by converting a transient loop-loop complex into a stable dimer. J. Biol. Chem. **271:**33686–33692.
52. **Muriaux, D., P. Fossé, and J. Paoletti.** 1996. A kissing complex together with a stable dimer is involved in the HIV-1_{Lai} RNA dimerization process in vitro. Biochemistry **35:**5075–5082.
53. **Muriaux, D., P.-M. Girard, B. Bonnet-Mathonière, and J. Paoletti.** 1995. Dimerization of HIV-1_{Lai} RNA at low ionic strength. An autocomplementary sequence in the 5′ leader region is evidenced by an antisense oligonucleotide. J. Biol. Chem. **270:**8209–8216.
54. **Murti, K. G., M. Bondurant, and A. Tereba.** 1981. Secondary structural features in the 70S RNAs of Moloney murine leukemia and Rous sarcoma viruses as observed by electron microscopy. J. Virol. **37:**411–419.
55. **Myers, G., B. Korber, B. H. Hahn, K.-T. Jeang, J. W. Mellors, F. E. McCutchan, L. E. Henderson, and G. N. Pavlakis.** 1995. Human retroviruses and AIDS: a compilation and analysis of nucleic acid and amino acid sequences. Los Alamos National Laboratory, Los Alamos, N.Mex.
56. **Paillart, J.-C., L. Berthoux, M. Ottmann, J.-L. Darlix, R. Marquet, B. Ehresmann, and C. Ehresmann.** 1996. A dual role of the putative RNA dimerization initiation site of human immunodeficiency virus type 1 in genomic RNA packaging and proviral DNA synthesis. J. Virol. **70:**8348–8354.
57. **Paillart, J.-C., R. Marquet, E. Skripkin, B. Ehresmann, and C. Ehresmann.** 1994. Mutational analysis of the bipartite dimer linkage structure of human immunodeficiency virus type 1 genomic RNA. J. Biol. Chem. **269:**27486–27493.
58. **Paillart, J.-C., E. Skripkin, B. Ehresmann, C. Ehresmann, and R. Marquet.** 1996. A loop-loop "kissing" complex is the essential part of the dimer linkage of genomic HIV-1 RNA. Proc. Natl. Acad. Sci. USA **93:**5572–5577.
59. **Parolin, C., T. Dorfman, G. Palu, H. Gottlinger, and J. Sodroski.** 1994. Analysis in human immunodeficiency virus type 1 vectors of *cis*-acting sequences that affect gene transfer into human lymphocytes. J. Virol. **68:**3888–3895.
60. **Parsons, J. T., P. Lewis, and P. Dierks.** 1978. Purification of virus-specific RNA from chicken cells infected with avian sarcoma virus: identification of genome-length and subgenomic-length viral RNAs. J. Virol. **27:**227–238.
61. **Peacock, A. C., and C. W. Dingman.** 1967. Resolution of multiple ribonucleic acid species by polyacrylamide gel electrophoresis. Biochemistry **6:**1818–1827.
62. **Ratner, L., W. Haseltine, R. Pataarca, K. J. Livak, B. Starcich, S. F. Josephs, E. R. Doran, J. A. Rafalski, E. A. Whitehorn, K. Baumeister, L. Ivanoff, S. R. Petteway, Jr., M. L. Pearson, J. A. Lautenberger, T. S. Papas, J. Ghrayeb, N. T. Chang, R. C. Gallo, and F. Wong-Staal.** 1985. Complete nucleotide sequence of the AIDS virus, HTLV-III. Nature **313:**277–284.
63. **Sakaguchi, K., N. Zambrano, E. T. Baldwin, B. A. Shapiro, J. W. Erickson, J. G. Omichinski, G. M. Clore, A. M. Gronenborn, and E. Appella.** 1993.

Identification of a binding site for the human immunodeficiency virus type 1 nucleocapsid protein. Proc. Natl. Acad. Sci. USA **90:**5219–5223.

64. **Salminen, M. O., B. Johansson, A. Sonnerborg, S. Ayehunie, D. Gotte, P. Leinikki, D. S. Burke, and F. E. McCutchan.** 1996. Full-length sequence of an Ethiopian human immunodeficiency virus type 1 (HIV-1) isolate of genetic subtype C. AIDS Res. Hum. Retroviruses **12:**1329–1339.
65. **Sambrook, J., E. F. Fritsch, and T. Maniatis.** 1989. Molecular cloning: a laboratory manual, 2nd ed. Cold Spring Harbor Laboratory Press, Cold Spring Harbor, N.Y.
66. **Skripkin, E., J.-C. Paillart, R. Marquet, M. Blumenfeld, B. Ehresmann, and C. Ehresmann.** 1996. Mechanisms of inhibition of in vitro dimerization of HIV type I RNA by sense and antisense oligonucleotides. J. Biol. Chem. **271:**28812–28817.
67. **Skripkin, E., J.-C. Paillart, R. Marquet, B. Ehresmann, and C. Ehresmann.** 1994. Identification of the primary site of the human immunodeficiency virus type 1 RNA dimerization *in vitro*. Proc. Natl. Acad. Sci. USA **91:**4945–4949.
68. **Vanden Haesevelde, M., J.-L. Decourt, R. J. De Leys, B. Vanderborght, G. Van der Groen, H. Van Heuverswijni, and E. Saman.** 1994. Genomic cloning and complete sequence analysis of a highly divergent African human immunodeficiency virus isolate. J. Virol. **68:**1586–1596.
69. **Vanden Haesevelde, M., M. Peeters, G. Jannes, W. Janssens, G. Van der Groen, P. M. Sharp, and E. Saman.** 1996. Sequence analysis of a highly divergent HIV-1-related lentivirus isolated from a wild captured chimpanzee. Virology **221:**346–350.
70. **Vicenzi, E., D. S. Dimitrov, A. Engelman, T.-S. Migone, D. F. J. Purcell, J. Leonard, G. Englund, and M. A. Martin.** 1994. An integration-defective U5 deletion mutant of human immunodeficiency virus type 1 reverts by eliminating additional long terminal repeat sequences. J. Virol. **68:**7879–7890.